

# A New Criterion for Automatic Phase Correction of High-Resolution NMR Spectra Which Does Not Require Isolated or Symmetrical Lines

GIUSEPPE BALACCO

Laboratori di Ricerca Chimica, A. Menarini Industrie Farmaceutiche Riunite S.r.l., Via Sette Santi, 3-50131 Florence, Italy

Received October 2, 1993; revised January 26, 1994

A new method called ZOE (zero-order equality) for automatic phase correction of routine FT-NMR spectra is proposed. Starting from the notion that the ratio between the integrals of a peak in the imaginary and in the real part of the spectrum is correlated to the phase of the peak, a function is constructed which goes to zero when the spectrum does not need first- or higher-order corrections. The root of this function can be rapidly found by iteration and furnishes the value for first-order phase correction. Also, an ancillary very fast peak-finding algorithm is proposed which is insensitive to phase distortions. Experimental results show that ZOE succeeds when other methods cannot be applied, the main requirements being a fair baseline and  $S/N$  ratio, which are often fulfilled in routine high-resolution  $^1\text{H}$  NMR (and not, for example, in the field of *in vivo* spectroscopy). Other requirements, such as phase errors of less than second order and phase differences within the peaks not greater than  $\pi$ , are usually met in high-resolution spectroscopy. © 1994 Academic Press, Inc.

where  $R_k$  and  $I_k$  are the real and imaginary components of data point  $k$ ,  $R'_k$  and  $I'_k$  are the new components after the correction,  $N$  is the number of points, and  $\alpha$  and  $\beta$  are the zero- and first-order phase correction parameters. These last two are found by the spectroscopist by trial and error (experience plays a major role here), and this is certainly the most general and maybe the most accurate way of finding them.

Many automatic methods have been proposed for finding  $\alpha$  and  $\beta$  by computer. They differ in the requirements they impose on the spectra to be processed. Some of them require a good baseline (2), others a Lorentzian shape for the peaks (3), and others the presence of at least two isolated and symmetric peaks (4, 5). Some of them are computationally very intense (6), while others require interaction with the user, so they are not truly automatic (7). Recently a new method has been presented which is claimed to be very robust and generally applicable (8). This method fits the phases of points at peak position with Eq. [3] (see below). Actually there is no theoretical evidence of the latter being tolerant of overlapping peaks; the authors themselves accept that extended overlap could represent a problem. Personal experience shows that the cited method is fooled by multiplets usually encountered in proton spectroscopy. In conclusion, the method presented in Ref. (8) is limited in applicability to *in vivo* spectroscopy, for which it was indeed devised.

In this paper, a new method is presented which is designed for routine high-resolution  $^1\text{H}$  spectra. It is deliberately tolerant of overlapping peaks and inhomogeneous magnetic fields (i.e., non-Lorentzian lineshapes). It has not been tested on *in vivo* spectra; theoretical considerations, however, would suggest that our approach is not suitable, because of the large baseline and phase distortions typical of *in vivo* spectroscopy.

## INTRODUCTION

Pulsed NMR spectra are usually displayed in their absorptive mode, which has the advantages over other presentations (such as dispersive, magnitude, or power spectrum) of higher resolution and proportionality between the peak integral and the number of nuclei which give rise to the signal. Spectra after Fourier transformation are not absorptive, because of experimental reasons (1). The resulting phase anomalies are easily cured by software, taking linear combinations of the real and imaginary parts of the spectrum. The correction generally applied is

$$R'_k = R_k \cos\left(\alpha + \frac{k}{N}\beta\right) - I_k \sin\left(\alpha + \frac{k}{N}\beta\right),$$

$$I'_k = R_k \sin\left(\alpha + \frac{k}{N}\beta\right) + I_k \cos\left(\alpha + \frac{k}{N}\beta\right),$$

$$k = 0 \cdots N - 1,$$

[1]

## THE ZOE CRITERION

An NMR spectrum in the time domain (a FID) is a complex quantity which can be expressed as a sum of damped sinusoids, each one with its own phase,

$$f(t) = \sum_j A_j \exp(i\omega_j t + \phi_j) g_j(t), \quad [2]$$

where  $A_j$ ,  $\omega_j$ , and  $\phi_j$  are, respectively, the intensity, the frequency, and the phase of each signal, while  $g_j(t)$  ideally is an exponential decay, giving rise to a Lorentzian lineshape in the frequency domain. Here we let  $g_j(t)$  be any reasonable real function.

Normally the phases are a linear function of the frequency

$$\phi_j = \Phi_0 + \frac{\omega_j}{N} \Phi_1. \quad [3]$$

Here and in the following we assume for simplicity that the frequency in the spectrum is measured in number of points, the minimum frequency being 0 and the maximum (equivalent to the spectral width) being  $N$ . Coefficients  $\Phi_0$  and  $\Phi_1$  are conceptually distinct from  $\alpha$  and  $\beta$  of Eq. [1], the former being part of an ideal model of the spectrum, while the latter are the corrections apported by the spectroscopist. For the spectrum to be correctly phased,  $\alpha$  and  $\beta$  should have, respectively, the values  $-\Phi_0$  and  $-\Phi_1$ .

In the limiting case where  $\Phi_1 = 0$ , all the frequency components add coherently at time  $t = 0$ , giving the complex quantity

$$f(0) = \exp(\Phi_0) \sum_j A_j g_j(0) = \sum_k F(k), \quad [4]$$

whose module is the sum of the (weighted) intensities and whose phase is just  $\Phi_0$ .

The second equality recalls a known relation between Fourier pairs, namely that the quantity  $F(0)$  is equivalent to the integrated area of the frequency-domain spectrum  $F(\omega)$ . Particularly, I define the angle  $\theta_{qq'}$  as the function

$$T_{qq'} = \frac{\sum_{k=q}^{q'-1} I_k}{\sum_{k=q}^{q'-1} R_k},$$

$$\theta = \arctan(T_{qq'}) \quad \text{for } \sum R > 0,$$

$$\theta = \arctan(T_{qq'}) + \pi \quad \text{for } \sum R < 0 \text{ and } T_{qq'} > 0,$$

$$\theta = \arctan(T_{qq'}) - \pi \quad \text{for } \sum R < 0 \text{ and } T_{qq'} < 0, \quad [5]$$

so that  $\theta_{0N}$  is equal to  $\Phi_0$  if and only if  $\Phi_1 = 0$ . At the same time, if the interval  $q \cdots q'$  completely encloses a single peak  $j$  and does not include any part of any other peak, then  $\theta_{qq'} = \phi_j$ .

The angle  $\theta_{0N}$  gives a quick but rough way of phase-correcting a spectrum, namely to multiply it by  $\exp(-i\theta_{0N})$ . This kind of correction, first suggested by Ernst (9), gives satisfactory results only if the spectrum is made up by a

single line; nonetheless, it ensures that the real part is nearer to absorption than the imaginary one. To be more precise, it ensures that at one frequency  $x$  (with  $0 \leq x < N$ ) the spectrum is correctly phased, and, since the phase at each point  $k$  is proportional to  $(k - x)$ , we can be sure that

$$\phi_k = \Phi_1 \frac{k - x}{N} < \Phi_1. \quad [6]$$

We shall see later that this is a good starting point for the ZOE algorithm.

Equation [4] shows a simple property of  $\Phi_1$ : If each point  $k$  of the spectrum were multiplied by  $\exp(-ik\Phi_1)$ , then all the peaks of the spectrum would have the same phase. The ZOE criterion is simply an arbitrary transposition of this property, which substitutes  $\beta$  for  $-\Phi_1$  and  $\theta_{qq'}$  for the phase of a peak. It can thus be stated, the optimal first-order phase correction  $\beta$ , when applied, would make equal the values of two  $\theta_{qq'}$  angles calculated over different intervals of the spectrum. That is, zero-order equality for the whole spectrum.

To understand how we can find  $\beta$  using ZOE, we shall first examine a hypothetical spectrum composed of two completely separated lines with frequency  $r$  and  $l$ , with  $r < l$ . Let us suppose that point  $m$  is in the flat region between these two peaks ( $r < m < l$ ). One can easily see that  $\theta_{0m}$  and  $\theta_{mN}$  now measure the distinct phases  $\phi_r$  and  $\phi_l$  of the two noninterfering peaks. If we apply a first-order phase correction  $\beta$  to the spectrum, point  $k$  will undergo the rotation described in Eq. [1] and  $\theta_{0m}$  and  $\theta_{mN}$  will also change. We can obtain their dependency on  $\beta$  by simply noting that the phase of each signal will vary according to

$$\phi_r(\beta) = \phi_r(0) + \beta \frac{r}{N},$$

$$\phi_l(\beta) = \phi_l(0) + \beta \frac{l}{N}. \quad [7]$$

For analogy,

$$\theta_{0m}(\beta) = \theta_{0m}(0) + \beta \frac{r}{N} \pm 2\pi p_r(\beta),$$

$$\theta_{mN}(\beta) = \theta_{mN}(0) + \beta \frac{l}{N} \pm 2\pi p_l(\beta). \quad [8]$$

Thus we have two linear dependencies, both with a positive slope (in particular,  $0 < \text{slope}_r < \text{slope}_l < 1$ ). The  $\theta$  functions can only assume values between  $\pm\pi$ , so if we are plotting the functions  $\theta$  versus  $\beta$ , these will be cyclically discontinuous at intervals  $2\pi N/r$  and  $2\pi N/l$  (note that these intervals are always larger than  $2\pi$ ). Figure 1 shows the typical saw-toothed shape of these functions. The function

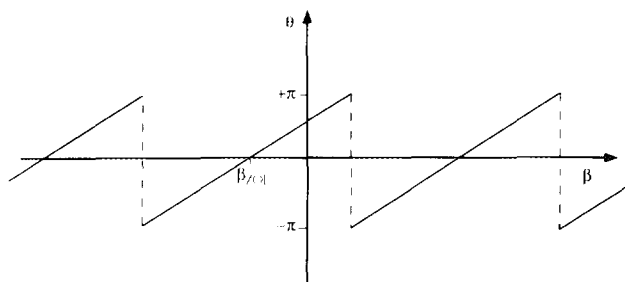


FIG. 1. The typical behavior of the functions  $\theta_{pp'}$  and  $\Delta\theta$  (see text).

$$\Delta\theta(\beta) = \theta_{mN} - \theta_{0m} = \Delta\theta(0) + \beta \frac{l-r}{N} \quad [9]$$

still resembles this shape, with slope  $(l-r)/N$  still contained in the interval  $0 \cdot \cdot \cdot 1$ , and also inherits the discontinuities of both functions [8].

According to the ZOE principle, the optimal first-order phase correction is obtained by equating the right sides of Eqs. [8],

$$\beta_{\text{ZOE}} = \Delta\theta(0) \frac{N}{r-l} = - \frac{\Delta\theta(0)}{\partial\Delta\theta/\partial\beta}. \quad [10]$$

Equation [10] suggests that  $\beta_{\text{ZOE}}$  can be computed from the starting values ( $\beta = 0$ ) of  $\Delta\theta$  and its first derivative respective to  $\beta$ . The value so found may be equal to or different from that given by the formula

$$\beta = - \frac{\phi_l - \phi_r}{l-r} N, \quad [11]$$

which could of course be used directly, but here we suppose that  $\phi_r$  and  $\phi_l$  cannot be measured.

In fact, function [10] has the infinite roots given by the formula  $\beta_{\text{ZOE}} \pm 2\pi(r-l)/N$ , while Eq. [11] gives only one "good" root. Care must be taken to avoid finding a spurious solution. In the first place, we can correct to zero order as suggested above, setting  $\alpha = -\theta_{0N}$ . This reduces the absolute values of  $\theta_{0m}(0)$  and  $\theta_{mN}(0)$ , pushing away the discontinuities from the point  $\beta = 0$  (see Fig. 1). If both  $\phi_r$  and  $\phi_l$  are less (in absolute value) than  $\pi$ , then we can be sure that Eqs. [10] and [11] give the same solution. For Eq. [6] this last condition holds necessarily if  $|\Phi_1| \leq \pi$  and is very likely to hold for bigger values, up to  $2\pi$ . In fact, if  $x$  in Eq. [6] is such that both  $(l-x)$  and  $(x-r)$  are not greater than  $N/2$ , this is exactly the validity range.  $\Phi_1$  originates mainly from the time lag  $\Delta t$  between the reading pulse and the start of acquisition and is theoretically predicted to be

$$\Phi_1 = \frac{2\pi\Delta t}{\text{dwell time}}. \quad [12]$$

This corresponds to a negative value for  $\beta$ . Knowing that, one could first apply a correction like  $\alpha = -\theta_{0N}$ ,  $\beta = -\pi$ , in order to increase by another  $\pi$  the range of applicability of ZOE. Even better, a rough estimate of  $\Phi_1$  can be done based on the values of  $\Delta t$  and of the spectral width. Normally this is not necessary, because  $\Phi_1$  is not so high; even when it is, strong first-order phase distortions have been shown to give a poor baseline (10), so it would be better to reduce  $\Delta t$  or to reconstruct the missing points through linear prediction (11, 12). Summarizing, the main prerequisite for applying ZOE is that all the peaks must have a phase less, in absolute value, than  $\pi$ ; this requisite can be easily satisfied.

Coming back to Eq. [10], this is not the safest way of finding  $\beta_{\text{ZOE}}$  numerically. Due to the low slope of  $\Delta\theta$ , a small imprecision in computing the derivative will lead to large deviations from the exact solution. We already know the sign of the derivative. So, starting from  $\beta = 0$ , we shall move away in fixed steps toward negative or positive values, respectively, if  $\Delta\theta$  is positive or negative, until the function changes sign. Figure 1 shows that going in the prescribed direction, the first root will always be met before the first discontinuity and that large steps up to  $\pi$  will bracket a root and never a discontinuity. Steps of  $\pi/2$  are a good compromise between speed and accuracy. Having restricted the solution in a range as large as the steps taken, one can obtain  $\beta$  by linear interpolation of the two extremes of this range. A further refinement substitutes the linear interpolation with the similar root-finding method known as "false position" (13). The latter is iterative but, due to the linear nature of the problem, is likely to converge in a very few steps (the precision needed is only on the order of  $10^{-2}$  rad). At this point the zero-order correction is simply given by

$$\alpha_{\text{ZOE}} = \frac{\theta_{0m}(\beta_{\text{ZOE}}) + \theta_{mN}(\beta_{\text{ZOE}})}{2}. \quad [13]$$

This example was developed only to derive the principal equations of the problem, but is not the one for which ZOE is designed. In fact, in such a simple case, a method like DISPA (4) would be faster and more accurate. Let us now consider the more general case where the point  $m$  completely divides not just two peaks, but two ensembles of (overlapping) peaks. Now not only do the  $\theta$ 's not correspond to the phases anymore, they are also not necessarily linear. Nonetheless, the previous discussion holds qualitatively and, in the proximity of the solution of Eq. [11] (i.e., in the absence of first-order phase distortions), even holds quantitatively because of Eq. [4]. Here again the ZOE criterion helps, suggesting that the solution of Eq. [10] should be the same as that of Eq. [11].

Even if the procedure described so far produces good results, it can be improved if  $\Delta\theta$  is redefined upon narrower intervals, that is, replacing Eq. [9] with

$$\Delta\theta(\beta) = \theta_{bb'} - \theta_{aa'} \quad [14]$$

The intervals  $a \cdots a'$  and  $b \cdots b'$  still enclose two different ensembles with  $0 < a < a' < b < b' < N$ . The advantages of the latter case are proximity to the ideal case of two single peaks, because the effect of  $\Phi_1$  is reduced in a narrower interval, speed of calculation, because the summations are taken over less points, and removal of the edges of a spectrum where baseline could be of concern because of the aliased tails of stronger peaks. Yet we need a way of obtaining the values of the four extremes. This is explained in the following section. Figure 2 represents the block diagram of a program based on the ZOE principle.

Although the requirement of two isolated ensembles of peaks is far less stringent than that of two isolated symmetrical singlets, it is still difficult to satisfy in  $^1\text{H}$  or  $^{31}\text{P}$  *in vivo* spectroscopy. This is another reason for restricting the range of applicability of ZOE to high-resolution spectra.

### THE PEAK-FINDING ALGORITHM

The aim of this algorithm is to find two intervals which completely enclose two distinct, distant, and isolated ensembles of peaks. It is composed of the following steps:

(1) The entire spectrum is divided into  $n$  regions 5 to 10 times as large as the average linewidth; typically  $n$  is a power of 2, ranging from 128 to 1024, whose exact value is not critical. Each region is characterized by a positive number  $\Delta$ , given by the difference between the tallest and lowest points, wherever they lie, in the real or in the imaginary part.  $\Delta$  is an inverse measure of the flatness of a region.

(2) The average  $\mu_B$  and standard deviation  $\sigma_B$  of the  $\Delta$ 's are calculated, where B stand for "baseline." The individual regions are then divided into the two categories of baseline ( $\Delta < \mu_B + 3\sigma_B$ ) and peaks ( $\Delta \geq \mu_B + 3\sigma_B$ ). The process is iterated over the remaining baseline regions until no  $\Delta$  in this category exceeds the quantity  $\mu_B + 3\sigma_B$ .

(3) The lowest- and highest-frequency regions classified as peaks are the starting basis for the desired intervals. They are extended to enclose all the contiguous regions whose  $\Delta$  is greater than the last calculated  $\mu_B$ .

(4) The intervals so found are further expanded until the condition is matched that the first extraneous regions have larger  $\Delta$  than the contiguous internal one.

This algorithm should ideally be applied to the dispersion spectrum, to encompass the larger spectral regions over which the long peaks' tails extend. The best which can be done is to consider simultaneously the real and imaginary part, so at worst we will examine a region misphased by only  $\pi/4$ .

The computational effort consists of  $2n$  additions, less than  $2n$  subtractions,  $n$  squares, and a few divisions. Since  $n$  is a small number, the algorithm is very efficient in computational speed. It also characterizes the baseline regions, giving

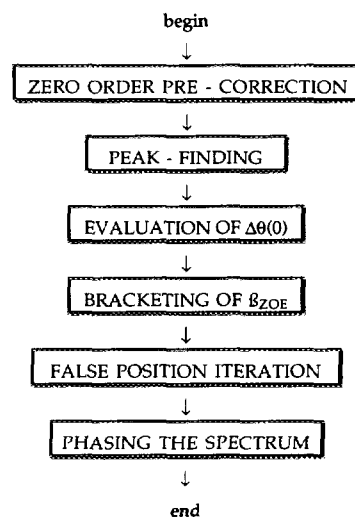


FIG. 2. Block diagram for a computer routine based on the ZOE criterion.

information which in turn can be used to baseline-correct the numerical integrals in Eq. [5]. Points just outside an interval can be used to estimate and correct the baseline in their proximity, provided that the interval is small compared to the spectral width, the interval is so large that its bounds are far from the internal peaks, and there are no other peaks nearby. The algorithm described can readily test if these conditions are matched by the intervals it has found.

### EXPERIMENTAL AND RESULTS

High-resolution  $^1\text{H}$  and  $^{13}\text{C}$  spectra of ethyl crotonate in  $\text{CDCl}_3$  were acquired on a Varian Gemini 200 CH spectrometer at 200 and 50 MHz, respectively. These spectra were chosen as representative of routine spectra of moderately concentrated samples in an organic chemistry department. Spectra were transferred to a Macintosh computer for processing with the SwaN-MR software package. The  $^1\text{H}$  4K FID was zero-filled to 8K, while a 2 Hz line broadening was applied to the  $^{13}\text{C}$  8K FID. Routines for ZOE automatic phasing were written in C and added to the SwaN-MR code. Phasing with the DISPA algorithm was accomplished with the built-in SwaN-MR command. This command requires the user to specify two reference peaks.

Figure 3a shows the spectrum of ethyl crotonate after FT, without phase correction. Although this spectrum has a good  $S/N$  ratio and little baseline distortion, it presents a challenge for many automatic and semiautomatic phasing algorithms, because of the absence of singlets and poor homogeneity of magnetic field. Figure 3b shows the best result which could be obtained with the DISPA algorithm, using the signal indicated by the arrows as reference signals. ZOE algorithm was first applied without the peak-finding routine, using Eq.

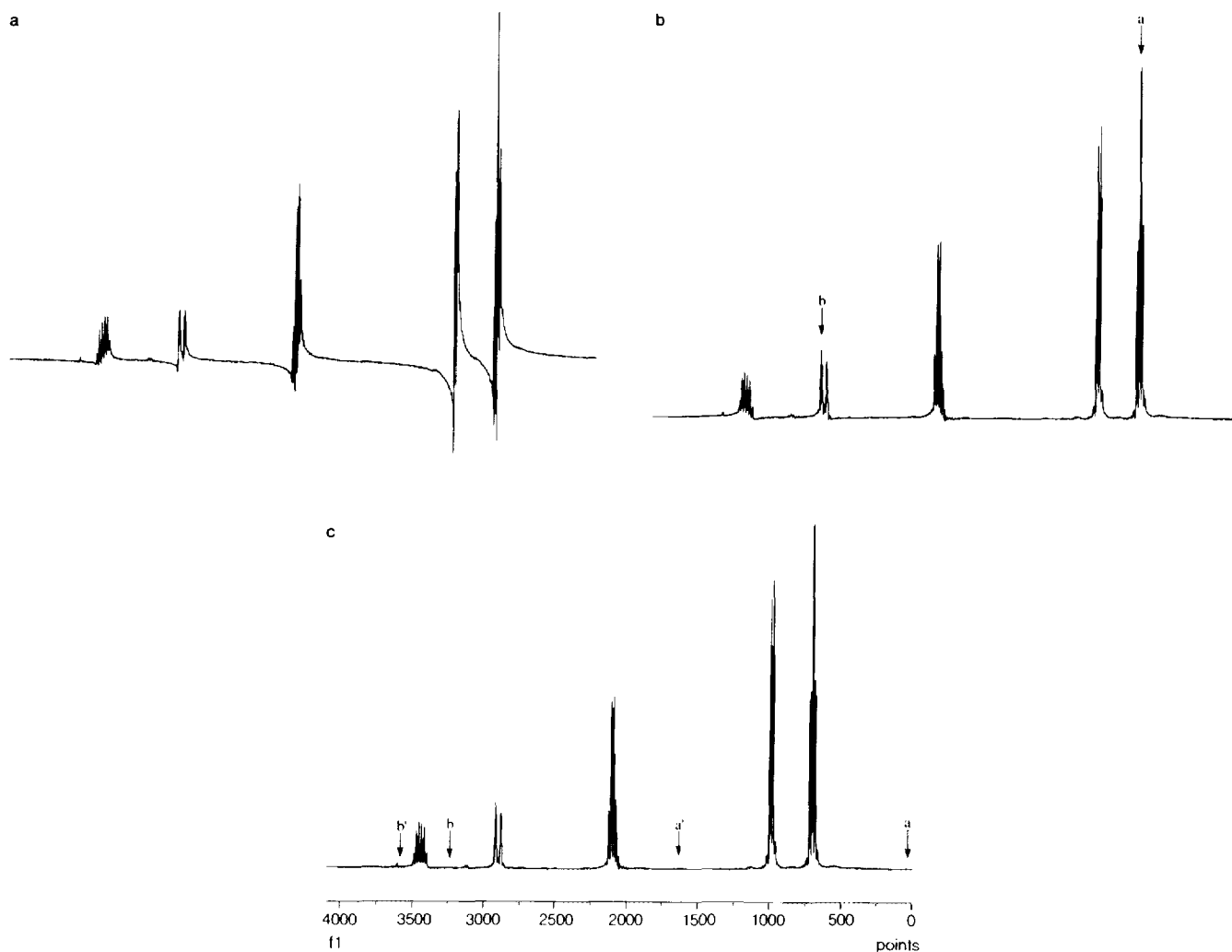


FIG. 3. (a) <sup>1</sup>H spectrum of ethyl crotonate without phase correction. (b) The spectrum corrected by the DISPA method. The arrows point to the reference peaks. (c) The spectrum after ZOE correction. The arrows indicate the frequencies as in Eq. [14] as determined by the automatic peak-finding routine.

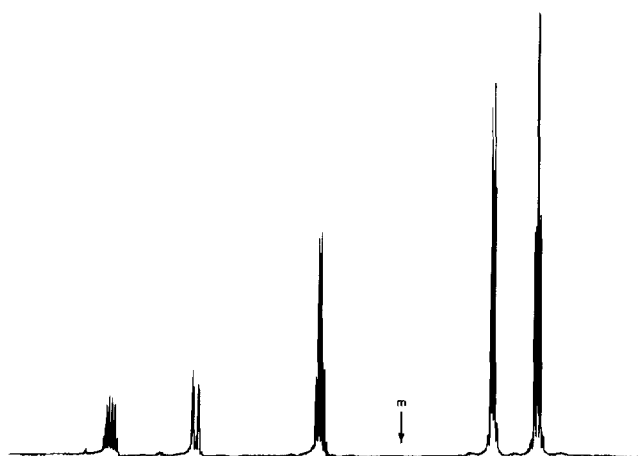


FIG. 4. The same as in Fig. 3c, but with the intervals of Eq. [9].

[8], with  $m$  directly supplied. The result is shown in Fig. 4, which is already superior to the DISPA result. Then the peak-finding routine was added, which gave the result shown in Fig. 3c. Time required was less than two seconds on a MC68030 computer running at 16 MHz. While the phase correction is constantly improving, correct phase for all the signals could be obtained only manually. Figure 5 shows the results obtained on the  $^{13}\text{C}$  spectrum of the same sample. Here the best results were obtained by the DISPA method, which proved to be the method of choice, while ZOE was misled by a peak with a very low  $S/N$  ratio. In this case of ZOE principle itself could have given better results if the peak-finding routine were more sophisticated.

The spectra were deliberately misphased to various extents and rephased using ZOE. The same results were consistently obtained if the first-order phase distortion was less than  $\pi$ . As predicted, with higher values the algorithm sometimes found a different solution. The sensitivity to bad baseline was tested. The first three complex points of the  $^1\text{H}$  FID were zeroed, producing a very distorted baseline. As could have

been expected, here DISPA continued to give better results. A baseline correction could not be introduced in the integration stage of ZOE, because the conditions outlined in the previous paragraph were not simultaneously satisfied. In other test spectra in which baseline correction was feasible, ZOE gave good results. In this case, a zero-order baseline correction is sufficient, that is, subtracting in the integrated interval the average of the outside points.

## CONCLUSION

My personal opinion is that manual phase correction still gives the most accurate results. Nonetheless, automatic routines can save much time by yielding an approximate solution. Results show that is difficult to find one method good for all seasons. In this respect, the different methods proposed in the literature can be divided into two classes: those which use all the spectrum (at least in the real part) and those which concentrate on the centers of taller peaks. While the former suffer from poor baseline and  $S/N$ , the latter are less

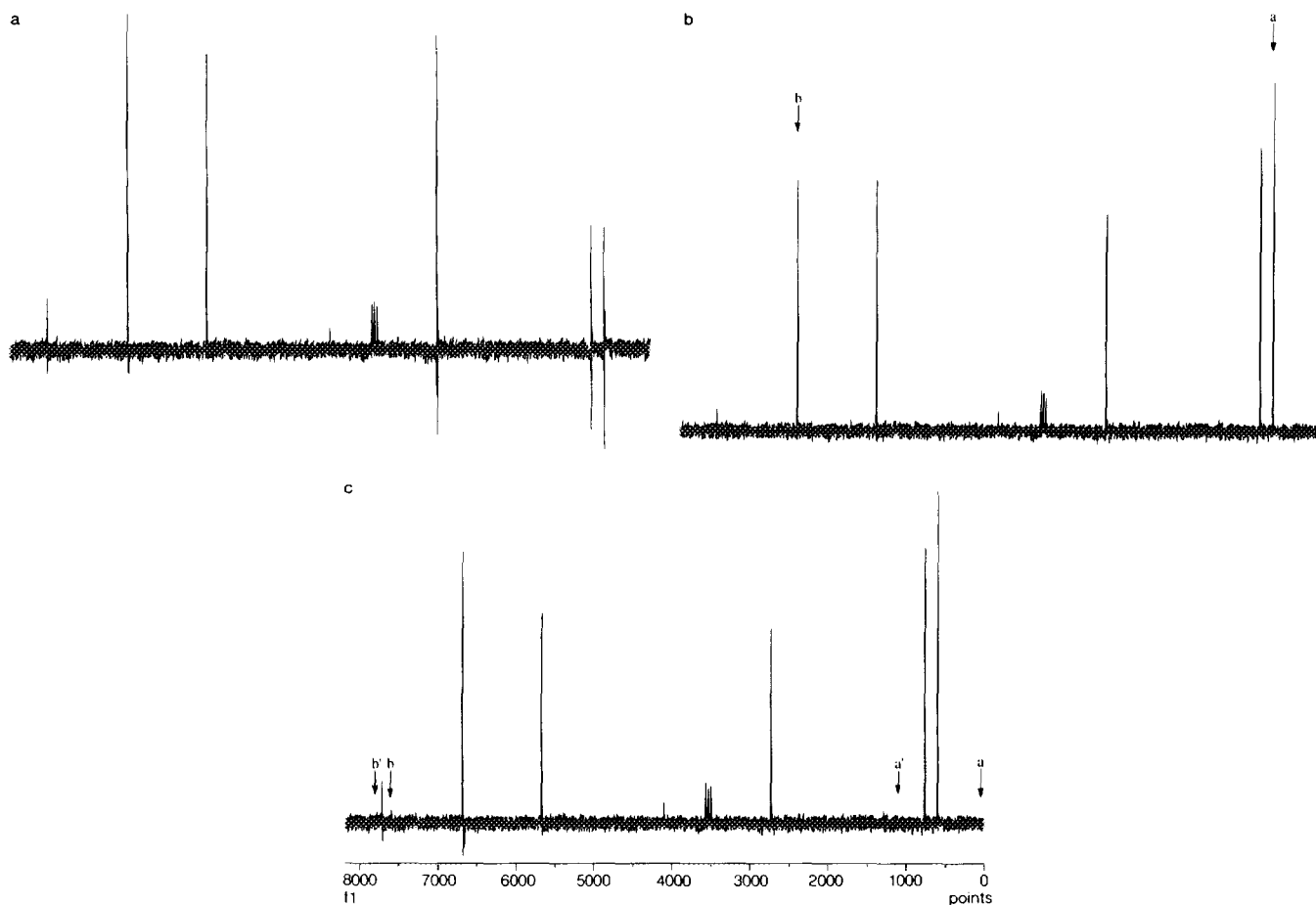


FIG. 5.  $^{13}\text{C}$  spectrum of ethyl crotonate without phase correction (a), with DISPA correction (b), and with ZOE correction (c). Arrows have the same meaning as those in Fig. 3.

tolerant of poor resolution, bad lineshapes, and peak overlap. The same two classes of methods have been so far differentiated by their numerical properties, the former being composed of iterative procedures, while the latter find their solution directly. Actually, many methods include an iterative procedure in one of their steps, e.g., full automatic DISPA (4). In this respect, ZOE represents an exception in the first class, in that the iterative root search is adopted only for numerical accuracy and is not intrinsic to the principle. Previous strategies, like the simplex method proposed by Siegel (14), blindly seek the maximum of a function to be optimized in two-dimensional space. ZOE not only requires less computing time, but is also less sensitive to the starting conditions and does not risk convergence to an erroneous local maximum. Finally, in favorable cases, even the baseline problem can be alleviated.

The method described in this paper was designed having in mind the spectra normally obtained inside a fine chemistry department and that was inevitably reflected in the limits of the method itself. So these limits must be carefully considered before trying to apply the ZOE principle in a different area.

#### ACKNOWLEDGMENT

I thank Antonio Guidi for reading this manuscript.

#### REFERENCES

1. E. Fukushima and S. B. W. Roeder, "Experimental Pulse NMR: A Nuts and Bolts Approach," p. 50, Addison-Wesley, Reading, Massachusetts, 1981.
2. D. E. Brown, T. W. Campbell, and R. N. Moore, *J. Magn. Reson.* **85**, 15 (1989).
3. F. Montigny, K. Elbayed, J. Brondeau, and D. Canet, *Anal. Chem.* **62**, 864 (1990).
4. C. H. Sotak, C. L. Dumoulin, and M. D. Newsham, *J. Magn. Reson.* **57**, 453 (1984).
5. A. Heuer, *J. Magn. Reson.* **91**, 241 (1991).
6. H. Barkhuijsen, R. de Beer, and D. van Ormondt, *J. Magn. Reson.* **61**, 465 (1985).
7. J. M. Daubenfield, J. C. Boubel, J. J. Delpuech, B. Neff, and J. C. Escalier, *J. Magn. Reson.* **62**, 195 (1985).
8. J. J. van Vaals and P. H. J. van Gerwen, *J. Magn. Reson.* **86**, 127 (1990).
9. R. R. Ernst, *J. Magn. Reson.* **1**, 7 (1969).
10. P. Plateau, C. Dumas, and M. Gueron, *J. Magn. Reson.* **54**, 46 (1983).
11. C. F. Tirendi and J. F. Martin, *J. Magn. Reson.* **81**, 577 (1989).
12. D. Marion and A. Bax, *J. Magn. Reson.* **83**, 205 (1989).
13. W. H. Press, B. P. Flannery, S. A. Teukolsky, and W. T. Vetterling, "Numerical Recipes," Chap. 9.2, Cambridge Univ. Press, New York, 1986.
14. M. M. Siegel, *Anal. Chim. Acta* **133**, 103 (1981).